

Supporting Information for

## **Linking the Surface and Subsurface in River Deltas - Part 2: Relating Subsurface Geometries and Groundwater Flow and Transport Behavior**

Zhongyuan Xu<sup>1</sup>, Jayaram Hariharan<sup>2</sup>, Paola Passalacqua<sup>2</sup>, Elisabeth Steel<sup>3</sup>, Chris Paola<sup>4</sup>, Holly A. Michael<sup>1,5\*</sup>

<sup>1</sup>Department of Earth Sciences, University of Delaware, Newark, Delaware, USA

<sup>2</sup>Department of Civil, Architectural and Environmental Engineering and Center for Water and the Environment, University of Texas at Austin, Austin, TX, USA

<sup>3</sup>Department of Geological Sciences and Geological Engineering, Queen's University, Kingston, Ontario, Canada

<sup>4</sup>Department of Earth and Environmental Sciences, University of Minnesota, Minneapolis, Minnesota, USA

<sup>5</sup>Department of Civil and Environmental Engineering, University of Delaware, Newark, Delaware, USA

Corresponding author: Holly A. Michael ([hmichael@udel.edu](mailto:hmichael@udel.edu))

### **Contents of this file**

Texts S1 to S3  
Figures S1 to S11  
Tables S1 to S2

### **Additional supporting information (Files uploaded separately)**

Input files for MODFLOW and MODPATH example simulation.

### **Introduction**

This supplementary document provides additional results and tests for numerical simulations and statistical analysis. The material is organized as three texts (Texts S1-S3), [eleven](#)

figures (Figures S1-S11) and two tables (Tables S1-S2). The validity test and test results of stitching method which is used in the groundwater model building are reported in Text S1, Table S1 and Figure S11. The groundwater model domain setup and parameter determination are reported in Text S2 and Figures S1-S3. The threshold value of hydraulic conductivity ( $K$ ) in binary model is determined in Text S3 and Figure S4. Further explanations of connectivity metrics, such as *connected geobody*, *percolated path*, *highest core sand fraction* and *fraction of high sand cores* are shown in Figures S5-S6. The division of three regions from upstream to downstream in delta models is shown in Figure S7. The overview of connectivity metrics vary with input sand fraction and rates of sea-level rise is shown in Figure S8-S10. Furthermore, the input files of MODFLOW and MODPATH codes are uploaded.

### **Text S1 Testing the stitching method.**

It is necessary to test the effect of our stitching method (Hariharan et al., submitted) on both static and dynamic connectivity to ensure that effects on results are minimal. The test compared connectivity metrics of raw cases (no stitching) and stitched cases by using high rates of sea-level rise (SLR) models. Four groups were considered: raw models, 2-section stitched models, 3-section stitched models and multi-section stitched models, where the total thickness of each model is the same, and components are individual pieces that are stitched together. Among them, multi-section models were used in this study, in which there are 5 to 10 model sections used in the stitching method. Table S1 shows the p-value of a T-test comparing metrics of raw models with three stitched models. For 6 out of 36 comparisons, the null hypothesis that there is no significant difference between two data sets is accepted. Figure S11 presents 6 significant difference comparisons and several insignificant difference comparisons. We think the general trend of dynamic behaviors is still kept in the stitched realizations, even they are significant different from raw realizations (Figure S11 d-f). Thus, we conclude that the stitching method is acceptable in this study.

### **Text S2. Groundwater model setup.**

The groundwater model domains were extracted from the DeltaRCM models so as to minimize statistical spatial non-stationarity. We chose a portion of each model domain that removes both the very sandy inlet section and the distal edges. Because the input parameters such as the SLR rate and ISF (input sand fraction) determine the size of the simulated delta and its stratigraphy, each realization is a different size. Therefore, the location of the extracted box is dependent on the size of delta.

In the strike direction, for clipping the sand accumulation in the inlet area, 30% of total sediment volume at the inlet was removed and 10% at the outlet was removed to create a rectangular volume (Figure S1a). In the dip direction, the box was taken on the middle 50% of total sediment volume (Figure S1a). For stitched models, the depth of the box was selected as 25 m. For raw models in the vertical direction, the top 5 m of sediment was removed to avoid scour holes caused by river erosion, and 7.5 m of sediment was removed from the bottom to avoid unrepresentative sand distributions caused by edge effects (Figure S1b). Therefore, each groundwater model is a different size, but large enough that there are many geologic features both horizontally, creating statistically stationary systems to the extent possible.

The model cutting also influenced the sand fraction in groundwater models. Because a large part of the downstream region was removed, the sand fraction of groundwater models was always larger than the corresponding ISF value (Figure 4). On the other hand, more river splitting in high SLR rate models caused more sand to accumulate in the inlet of delta, which was removed in model cutting. This resulted in a decrease in sand fraction with SLR rate (Figure 4 & Figure 5 & Figure S8a).

We converted sand content to hydraulic conductivity in each model. DeltaRCM records the proportions of sand and mud. We used the geometric mean of sand and mud proportion to convert sand content to hydraulic conductivity ( $K$ ) values. This method gives a very similar result to the Sauerbrei method (Vukovic & Soro, 1992; Devlin, 2015), but maintains continuity at extremely high and low sand content, the equation is shown below. The relationship of sand content and hydraulic conductivity is displayed in Figure S3.

$$K = (ps+pm)\sqrt{K_s^{ps} K_m^{pm}}$$

$K$  is the hydraulic conductivity of the specific cell;  $K_s$  is the hydraulic conductivity of sand,  $K_m$  is the hydraulic conductivity of mud;  $ps$  and  $pm$  are the proportion of sand and mud.

**Text S3 Threshold in binary system.**

Several static metrics in this study are based on a binarized representation, that is, the hydraulic conductivity field is divided into two parts by setting a threshold (Figure 2). The threshold in this study is defined as 0.8 sand content, for two reasons. First, most of the cells in the DeltaRCM models were either pure sand or mud (1 or 0), and the 70% input sand models contain a large number of cells with greater than 0.8 sand content (Figure S4). Second, in the advective transport modeling, most trajectories of fastest particles are the cells with sand content  $> 0.8$  both horizontally and vertically (Figure S4). The fastest particles are defined as the first 5% to arrive at the downstream boundary. This illustrates that preferential flow tends to occur in the connected pure-sand cells, and defining 0.8 as the threshold allows the static connectivity metrics to capture the preferential flow behavior.

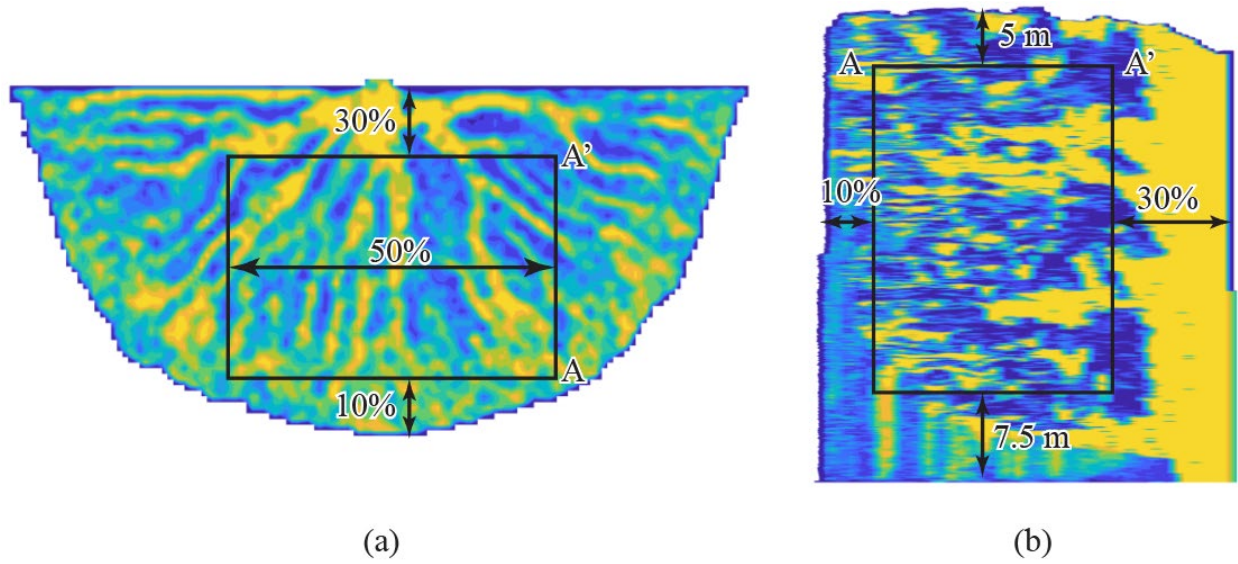


**Figure S1.** Box cutting from the numerical delta. (a) Plan view of the box. (b) Side view of the box cut in high-SLR rates (40-60 mm/y). The depth of stitched models (low-SLR rates, 0-30 mm/y) is determined as 25 m.

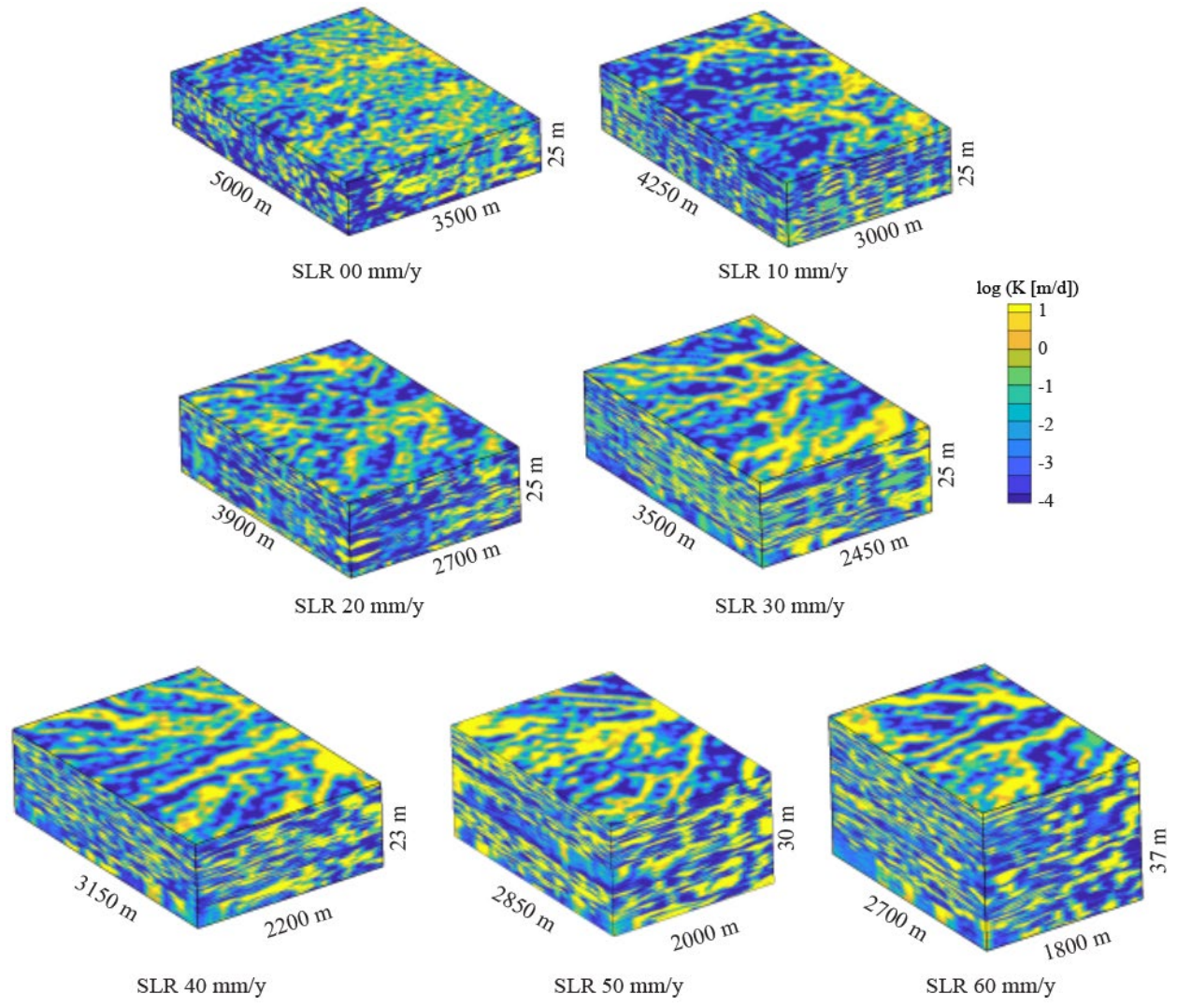


**Figure S2.** Sizes of groundwater domains under different rate of SLR scenarios, 30% ISF.

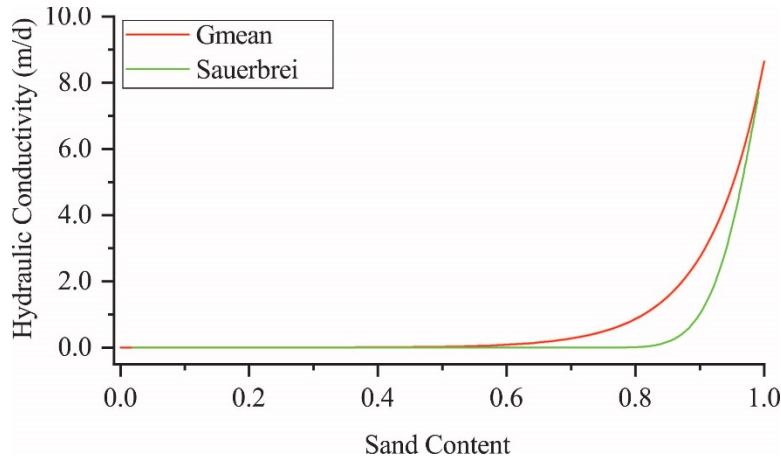


**Figure S3.** Conversion of sand content to hydraulic conductivity by geometric mean method and Sauerbrei Equation.

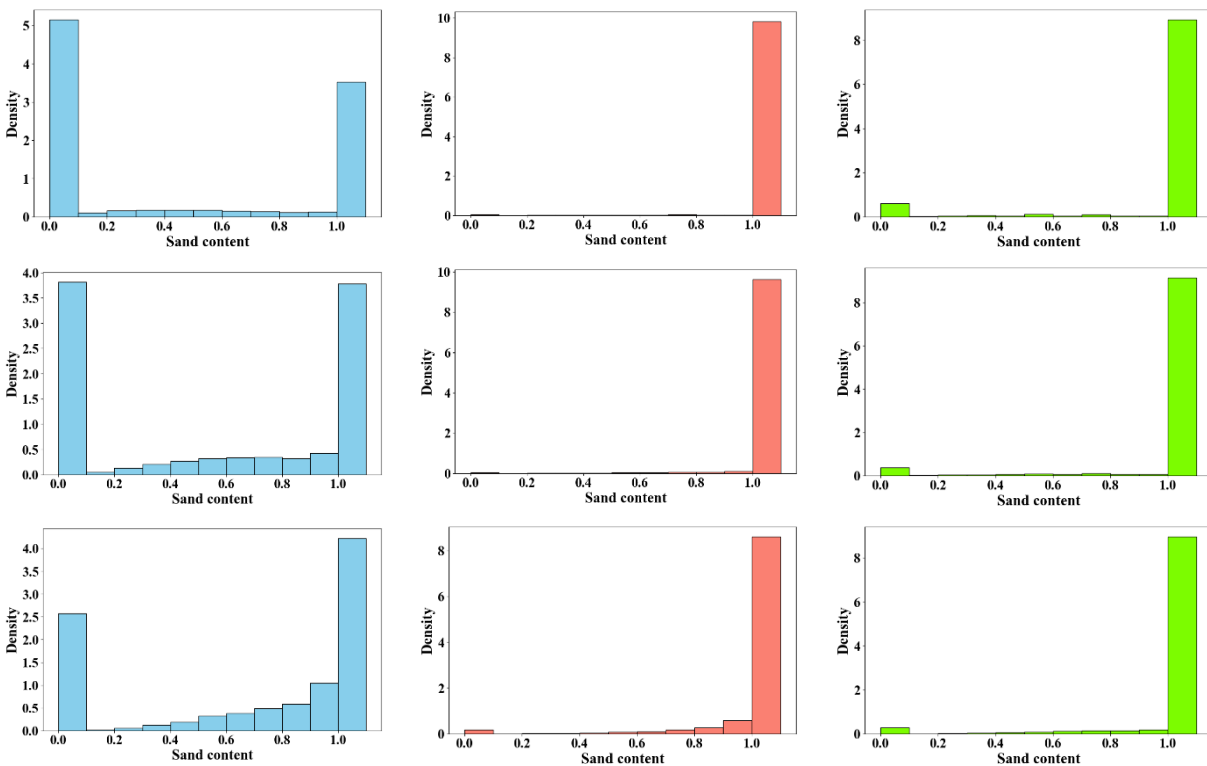


**Figure S4.** Sand fraction distribution of the whole system and trajectories of preferential flow. From top to bottom are data of ISF = 30%, 50%, 70% respectively. Histogram of blue (left) is sand content distribution of the whole system, histogram of red (middle) is sand content distribution of preferential trajectories on horizontal direction, histogram of green (right) is sand content distribution of preferential trajectories on vertical direction.

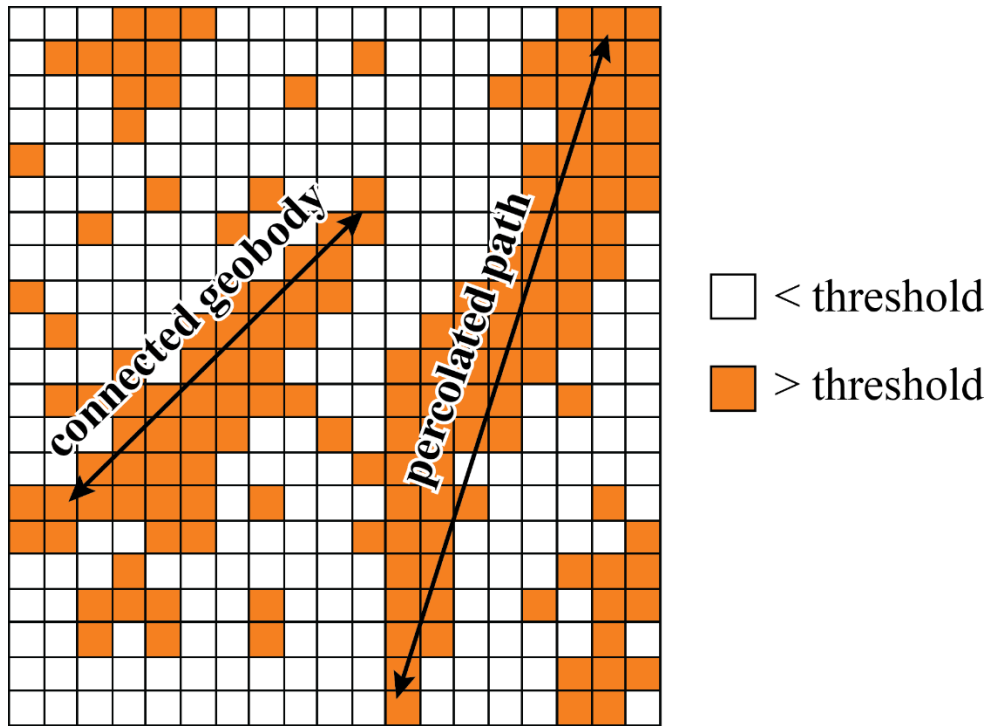


**Figure S5.** The definitions of geobody and percolated path used in the static metric calculations. Orange cells have parameter values of the cell greater than the threshold. A group of connected orange cells is defined as a geobody. A geobody that connects the upstream and downstream boundaries is defined as a percolated path.

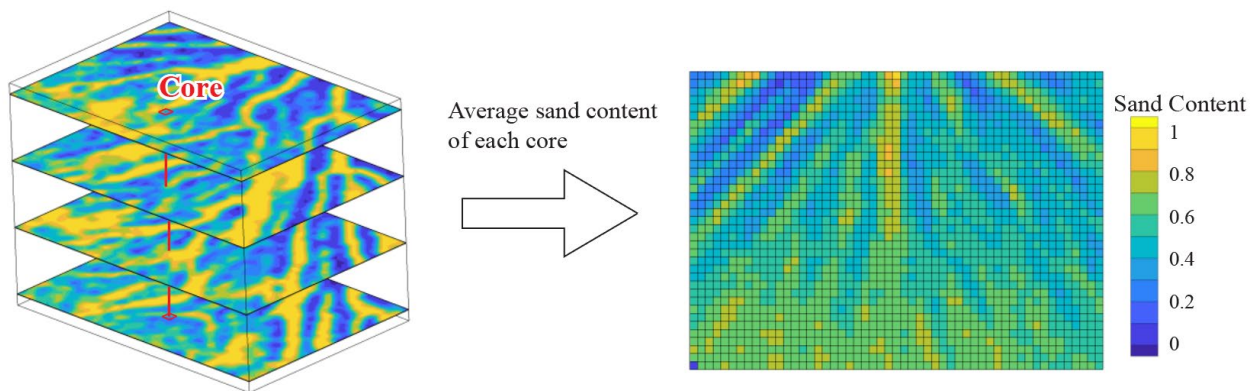


**Figure S6.** Converting the 3D data box to a 2D map by averaging sand content in each core.

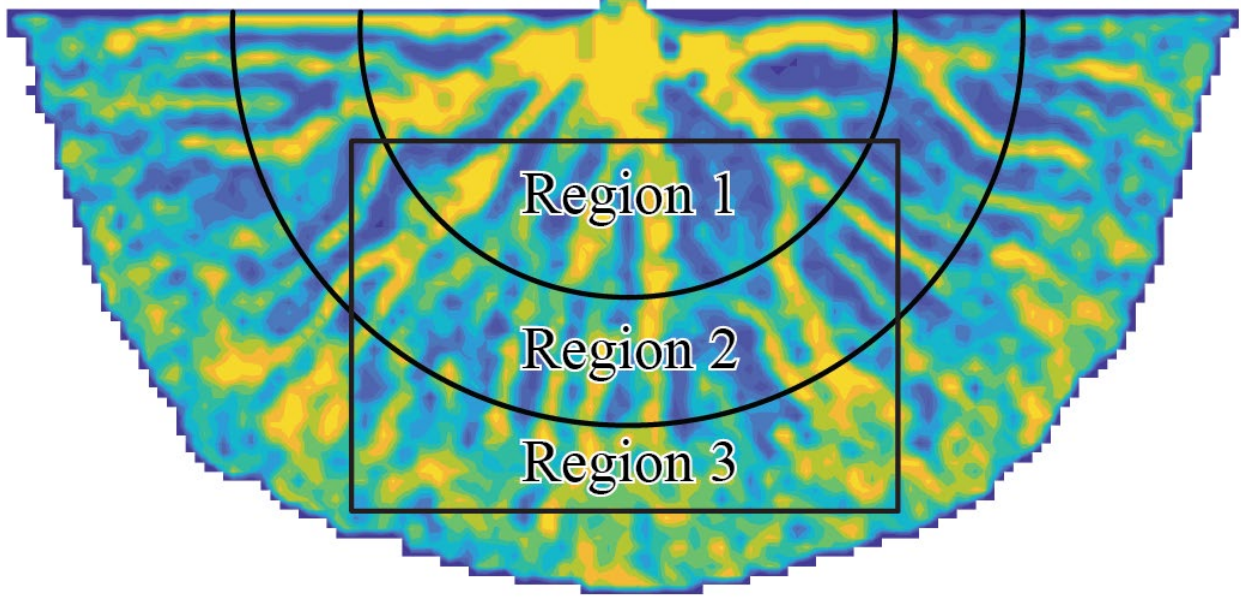


**Figure S7.** The study area was divided into 3 regions from upstream to downstream. The division is based on distance from sediment source. The local static metrics were calculated on the 3 regions.

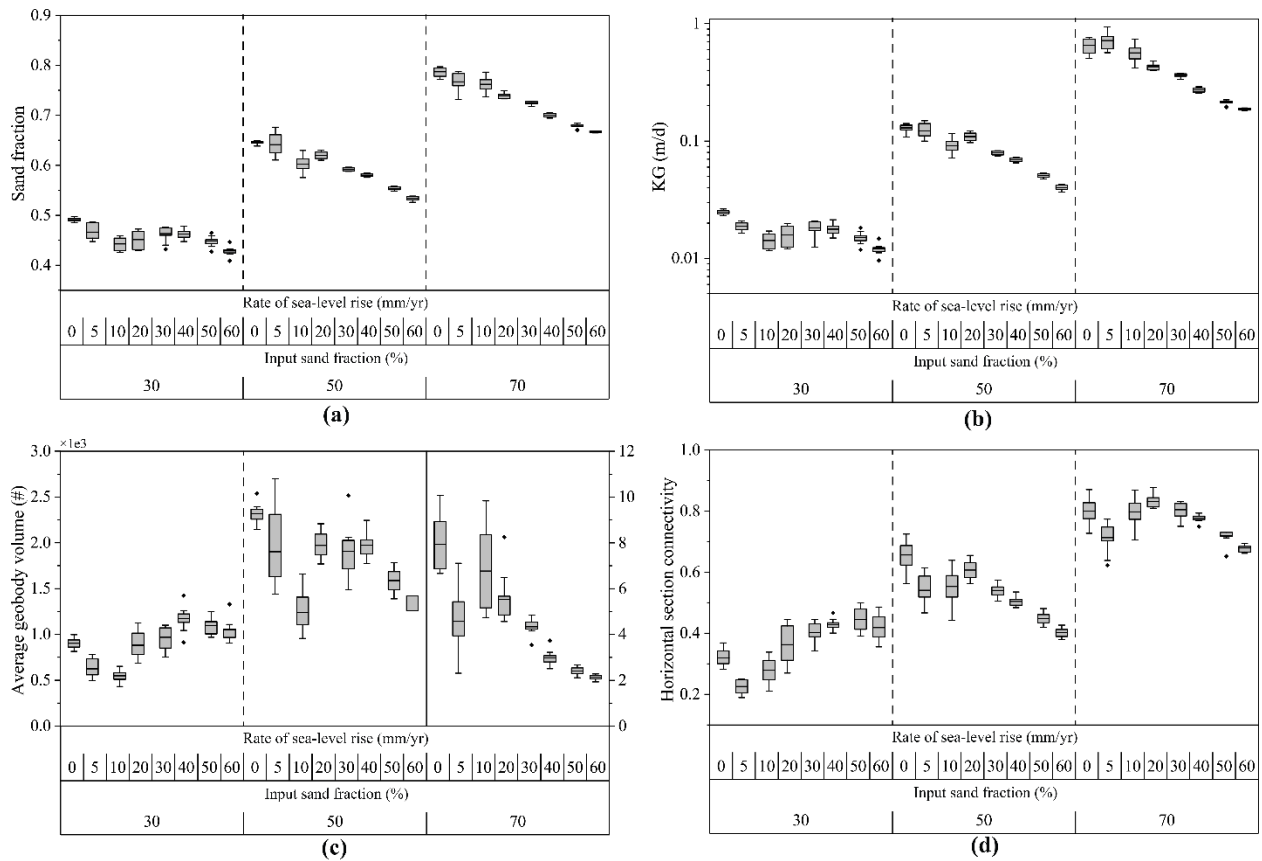


**Figure S8.** Static metrics under different input sand fractions and rates of sea-level rise (continue)

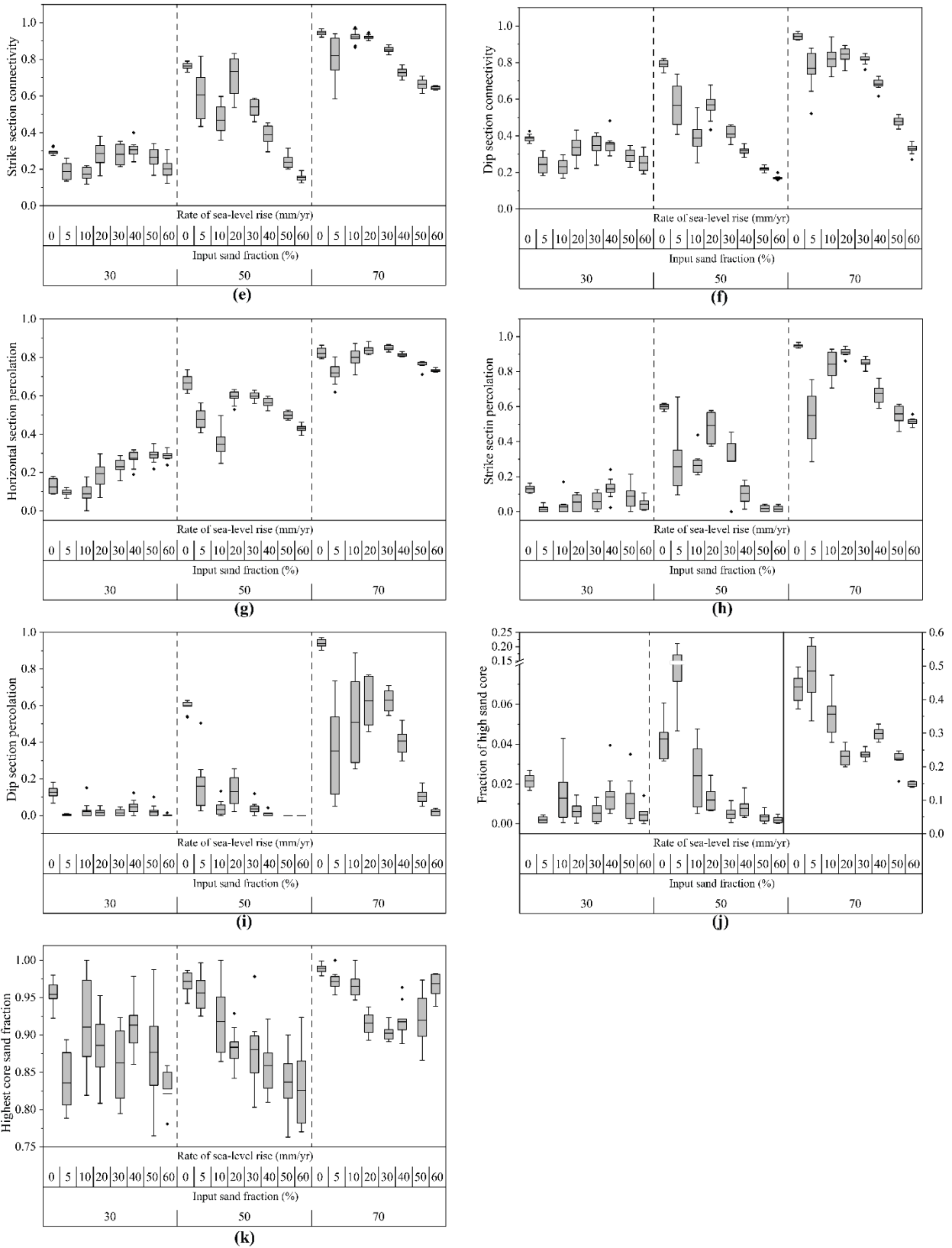


**Figure S8.** Static metrics under different input sand fractions and rates of sea-level rise

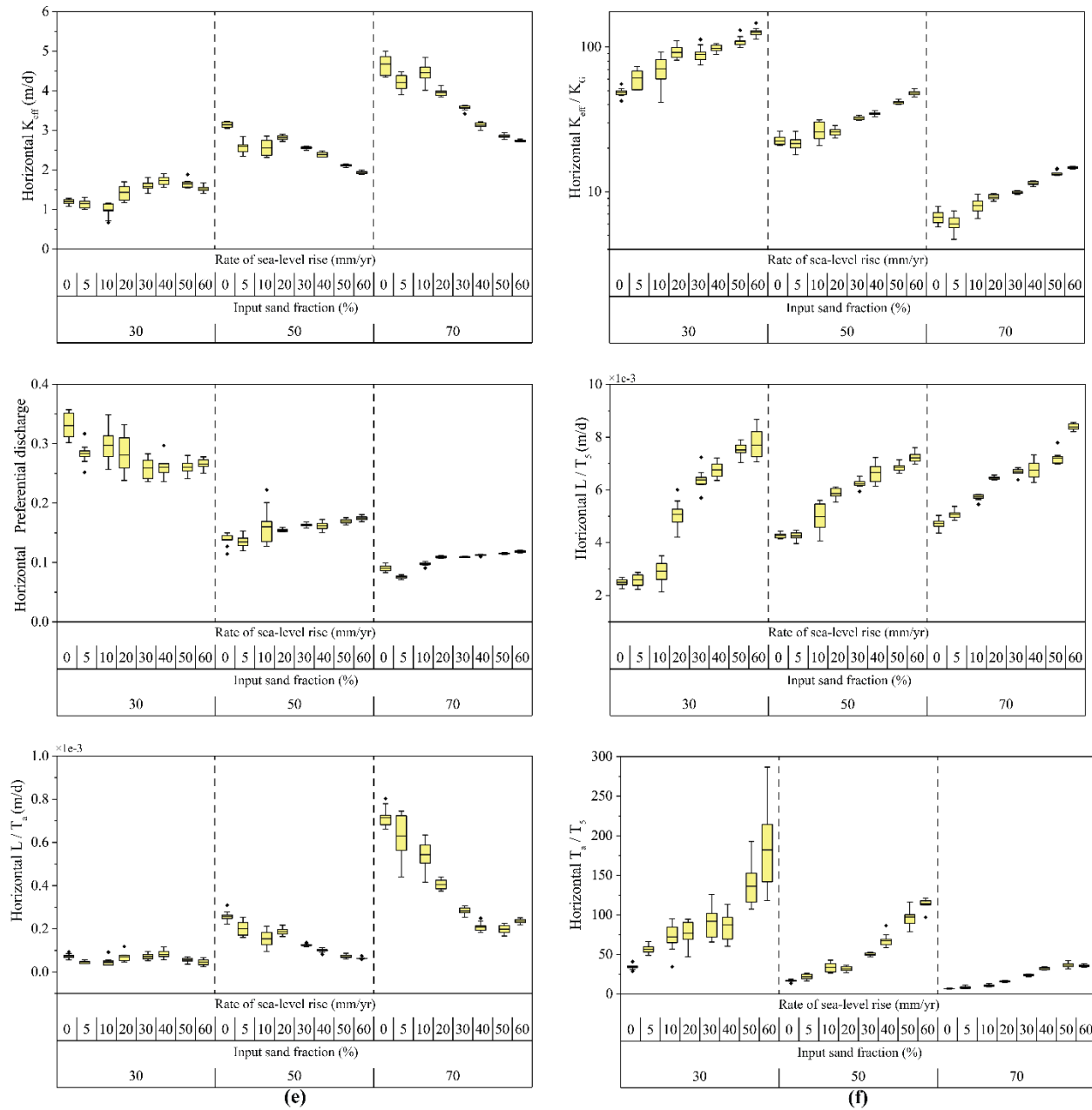


**Figure S9.** Horizontal dynamic metrics under different input sand fractions and rates of sea-level rise

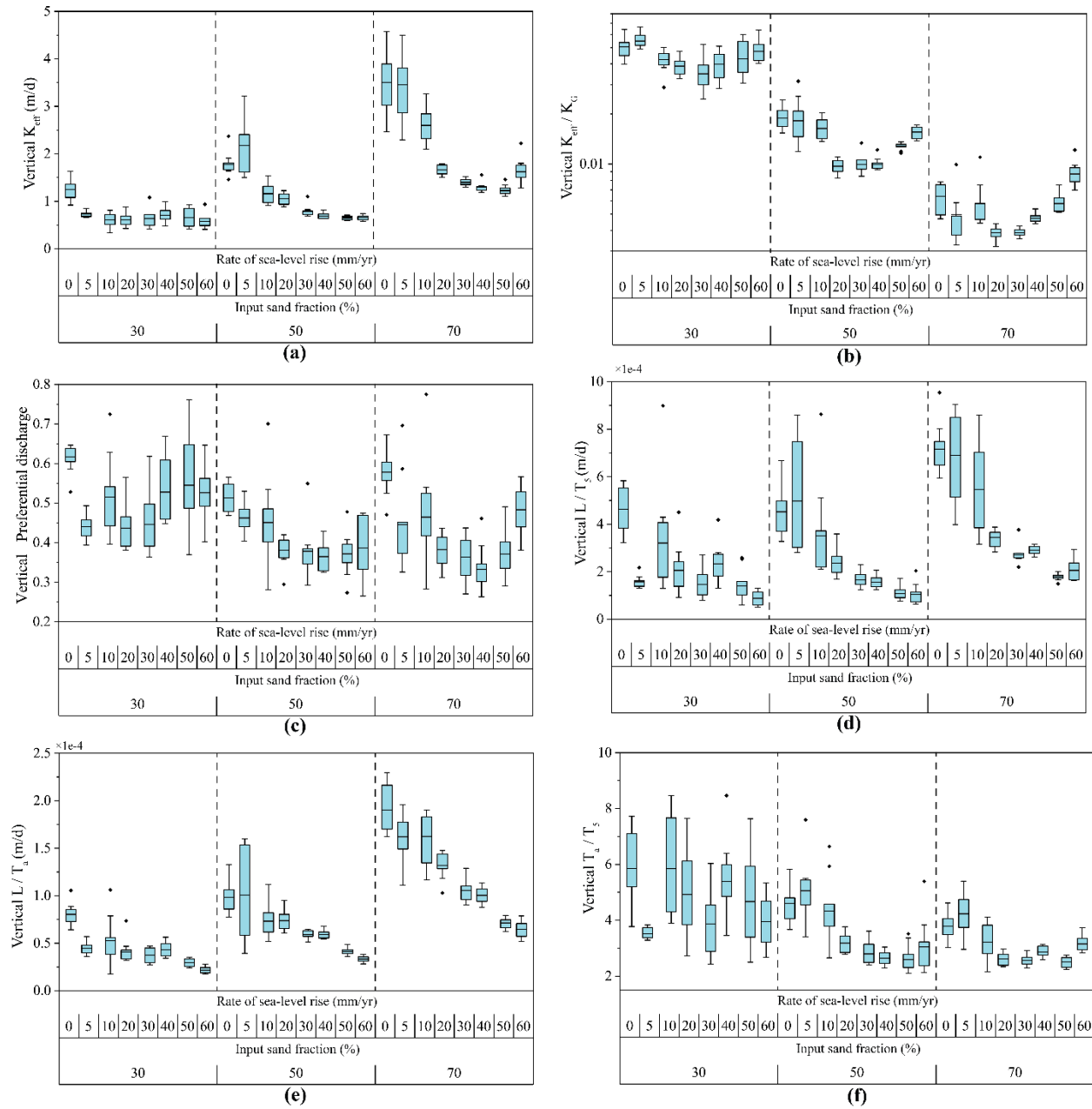


**Figure S10.** Vertical dynamic metrics under different input sand fractions and rates of sea-level rise

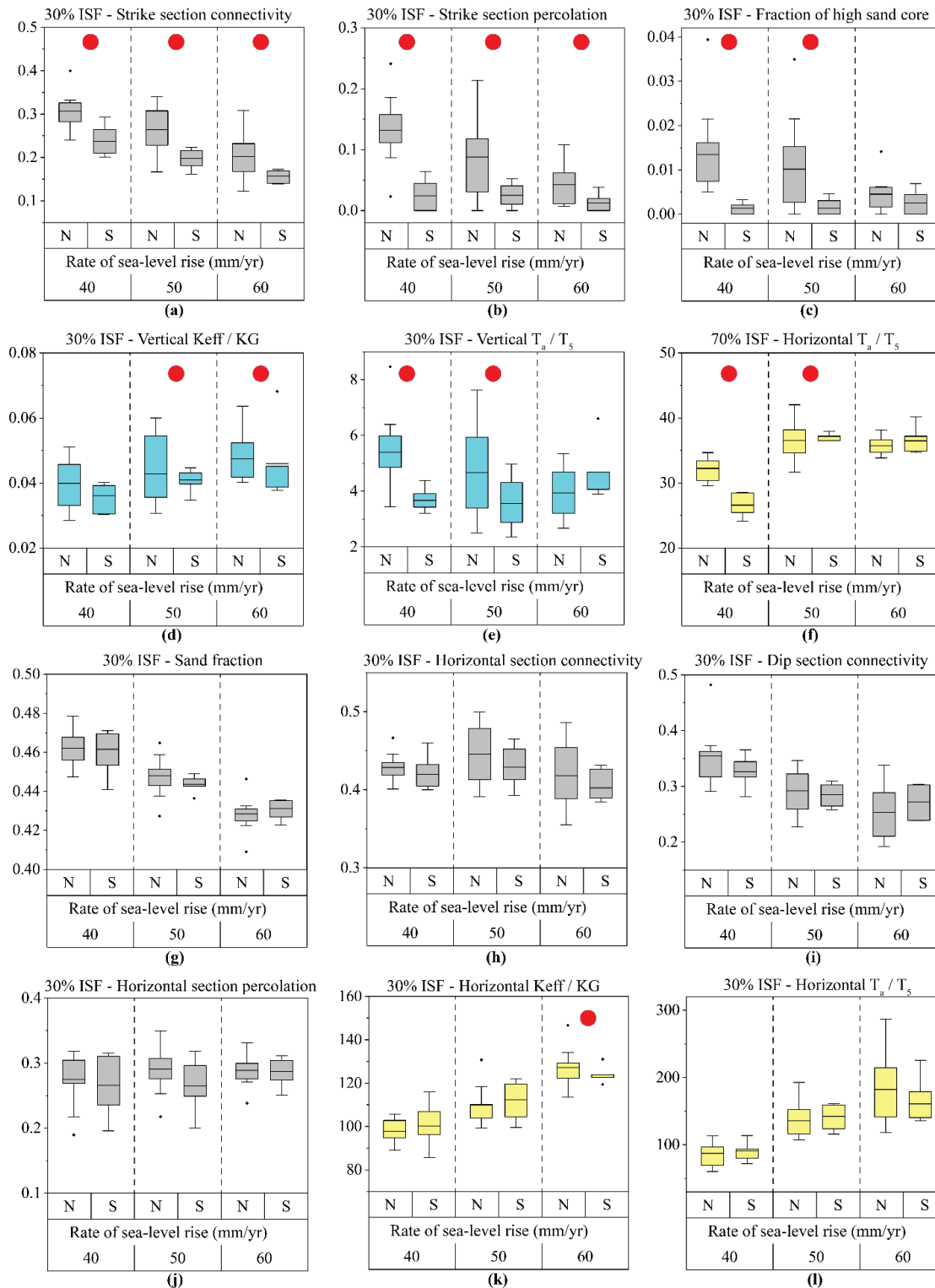


**Figure S11** Comparisons of non-stitched and stitched models. In the plot, N represents non-stitched (raw) models, S represents multiple sections (5-8) stitched models. **a-f** are plots where some significant differences occur (red values in Table S1, fifth column), **g-l** are several insignificant difference comparisons. Significantly different pairs are labeled with a red circle.

**Table S1.** Statistical tests for comparison of raw models with 2-section, 3-section and multiple-section stitched models in both static and dynamic metrics. The test statistic (p-value) was calculated by a two-sample t-test. Numbers in bold font indicate significance level > 95% (p-value < 5%) that two data sets are significantly different.

ISF	Metric	2 sections	3 sections	Multiple sections
30%	Sand Fraction	7.7e-1	4.3e-1	8.2e-2
	Average Geobody Volume	3.8e-1	7.3e-2	6.4e-2
	Horizontal Section Connectivity	4.4e-1	2.4e-1	2.4e-1
	Strike Section Connectivity	<b>4.5e-2</b>	7.9e-1	<b>2.8e-3</b>
	Horizontal Section Percolation	5.5e-1	4.5e-1	4.3e-1
	Strike Section Percolation	<b>3.3e-2</b>	2.9e-1	<b>2.3e-3</b>
	Highest Core Sand Fraction	5.2e-1	5.1e-1	1.3e-1
	Fraction of High Sand Core	6.0e-1	<b>2.5e-2</b>	<b>3.5e-4</b>
	Horizontal $K_{eff}/K_G$	9.8e-1	1.5e-1	4.9e-1
	Vertical $K_{eff}/K_G$	<b>2.8e-2</b>	<b>4.4e-2</b>	<b>1.3e-2</b>
	Horizontal $T_a/T_5$	4.1e-1	2.9e-1	5.1e-1
Vertical $T_a/T_5$	2.0e-1	7.8e-1	<b>1.5e-3</b>	
50%	Sand Fraction	5.3e-1	3.5e-1	7.2e-1
	Average Geobody Volume	2.4e-1	2.5e-1	9.6e-1
	Horizontal Section Connectivity	5.3e-1	6.0e-1	7.4e-2
	Strike Section Connectivity	7.9e-1	8.1e-1	6.9e-1
	Horizontal Section Percolation	8.5e-1	9.7e-1	1.9e-1
	Strike Section Percolation	3.9e-1	4.5e-1	8.1e-1
	Highest Core Sand Fraction	6.6e-1	8.0e-1	6.3e-1
	Fraction of High Sand Core	8.6e-1	3.0e-1	8.6e-1
	Horizontal $K_{eff}/K_G$	2.1e-1	1.6e-1	2.4e-1
	Vertical $K_{eff}/K_G$	3.7e-1	5.8e-1	4.3e-1
	Horizontal $T_a/T_5$	1.6e-1	2.7e-1	6.8e-2
Vertical $T_a/T_5$	8.5e-1	1.4e-1	8.4e-1	
70%	Sand Fraction	5.5e-1	5.3e-1	7.4e-1
	Average Geobody Volume	4.1e-1	3.8e-1	4.3e-1
	Horizontal Section Connectivity	7.5e-1	9.4e-1	5.6e-1
	Strike Section Connectivity	6.5e-2	2.5e-1	8.1e-2
	Horizontal Section Percolation	5.4e-1	4.6e-1	2.1e-1
	Strike Section Percolation	7.1e-2	3.5e-1	2.6e-1
	Highest Core Sand Fraction	8.8e-2	6.3e-1	1.0e-1
	Fraction of High Sand Core	3.2e-1	3.5e-1	4.4e-1
	Horizontal $K_{eff}/K_G$	2.4e-1	2.8e-1	4.5e-1
	Vertical $K_{eff}/K_G$	8.1e-1	3.9e-1	5.6e-1
	Horizontal $T_a/T_5$	2.0e-1	3.2e-1	<b>3.1e-2</b>
Vertical $T_a/T_5$	8.7e-2	2.3e-1	3.6e-1	

**Table S2.** The correlations between dynamic metrics and static metrics on the horizontal and vertical direction. 21 conditions are considered in each pair of metrics. The results are based on the P-value in Pearson Correlation which is less than 0.05. The bold font represents relatively high correlations.

Static \ Dynamic	Horizontal direction					Vertical direction				
	$K_{eff}$	$K_{eff}/K_G$	$L/T_5$	$L/T_a$	$T_a/T_5$	$K_{eff}$	$K_{eff}/K_G$	$L/T_5$	$L/T_a$	$T_a/T_5$
Sand fraction	<b>21</b>	<b>20</b>	7	9	8	3	4	0	3	2
Sand fraction in Region 1	12	11	8	11	9	5	3	1	2	4
Sand fraction in Region 2	10	11	6	6	6	5	4	0	1	1
Sand fraction in Region 3	9	10	4	6	6	2	3	1	1	2
$K_G$	<b>20</b>	<b>22</b>	6	8	8	2	4	0	1	2
$K_G$ in Region 1	12	10	6	10	11	5	4	2	2	4
$K_G$ in Region 2	11	10	5	6	3	4	3	1	1	1
$K_G$ in Region 3	10	9	4	5	5	2	3	1	0	2
Average geobody volume	15	10	5	9	8	4	2	1	3	1
Average geobody volume in Region 1	7	4	4	4	5	6	3	6	5	5
Average geobody volume in Region 2	6	6	5	6	5	3	2	1	0	3
Average geobody volume in Region 3	5	4	6	6	5	3	3	2	1	2
Horizontal section connectivity	<b>13</b>	<b>12</b>	6	8	7	4	5	2	2	3
Horizontal section connectivity in Region 1	8	8	7	9	6	6	5	3	2	5
Horizontal section connectivity in Region 2	9	7	4	3	4	6	5	2	1	3
Horizontal section connectivity in Region 3	5	7	3	3	3	2	5	3	0	1
Strike section connectivity	8	4	6	5	6	4	5	5	5	3
Strike section connectivity in Region 1	6	6	5	5	6	6	2	3	4	3
Strike section connectivity in Region 2	7	3	6	4	4	6	3	2	2	1
Strike section connectivity in Region 3	5	4	5	1	3	4	4	3	0	0
Dip section connectivity	9	6	4	7	8	6	2	2	3	3
Dip section connectivity in Region 1	7	3	2	3	1	5	4	3	2	3
Dip section connectivity in Region 2	6	4	5	4	2	6	3	2	0	1
Dip section connectivity in Region 3	4	4	2	3	1	5	4	2	1	0
Horizontal section percolation	<b>16</b>	7	<b>12</b>	6	4	5	5	2	3	2
Horizontal section percolation in Region 1	11	8	9	10	9	4	4	1	1	3
Horizontal section percolation in Region 2	11	9	5	8	5	5	4	2	3	3
Horizontal section percolation in Region 3	10	5	7	6	3	4	4	3	2	1
Strike section percolation	3	3	5	5	3	11	7	7	4	3

Strike section percolation in Region 1	5	2	4	6	3	7	5	4	4	2
Strike section percolation in Region 2	2	1	3	1	2	4	4	4	1	2
Strike section percolation in Region 3	3	3	4	0	1	5	5	4	0	2
Dip section percolation	5	2	1	4	3	12	10	7	2	7
Dip section percolation in Region 1	5	3	3	3	2	7	8	6	4	5
Dip section percolation in Region 2	3	2	4	2	1	6	4	4	2	3
Dip section percolation in Region 3	4	3	2	2	0	4	3	2	0	1
Highest core sand fraction	0	5	1	3	5	13	12	13	6	10
Highest core sand fraction in Region 1	0	5	1	2	4	13	11	11	5	9
Highest core sand fraction in Region 2	2	1	2	1	3	9	8	8	1	6
Highest core sand fraction in Region 3	2	3	5	1	0	4	4	5	2	3
Fraction of high sand core	6	9	4	4	2	12	9	11	4	9
Fraction of high sand core in Region 1	2	2	3	4	3	13	11	12	4	10
Fraction of high sand core in Region 2	5	2	2	1	1	6	4	6	4	5
Fraction of high sand core in Region 3	6	6	2	2	2	5	5	4	3	2